



# Forest beta-diversity analysis by remote sensing: How scale and sensors affect the Rao's Q index

Siddhartha Khare<sup>a</sup>, Hooman Latifi<sup>b,c,\*</sup>, Sergio Rossi<sup>a,d</sup>

<sup>a</sup> Département des Sciences Fondamentales, Université du Québec à Chicoutimi, Saguenay, QC, Canada

<sup>b</sup> Department of Photogrammetry and Remote Sensing, Faculty of Geodesy and Geomatics Engineering, K. N. Toosi University of Technology, Tehran, Iran

<sup>c</sup> Department of Remote Sensing, University of Würzburg, Germany

<sup>d</sup> Key Laboratory of Vegetation Restoration and Management of Degraded Ecosystems, Guangdong Provincial Key Laboratory of Applied Botany, South China Botanical Garden, Chinese Academy of Sciences, Guangzhou, China

## ARTICLE INFO

### Keywords:

Rao's Q and Shannon indices  
Invasive species  
Biodiversity  
Beta-diversity  
Remote sensing  
Pléiades 1A  
RapidEye  
Landsat-8

## ABSTRACT

Space-borne remote sensing missions provide robust, timely and continuous data to assess biodiversity in remote or protected areas, where direct field observations can be prohibited by difficult accessibility. The objective of this study was to extend the concept of remote sensing based assessment of beta-diversity to multi-scale domain by multi-resolution optical satellite data. This study was conducted in a reserved forest of western Himalaya, India; a region affected by the invasive *Lantana camara* L (lantana). We calculated and compared Rao's Q and Shannon indices at different spatial resolutions (0.5, 5, and 30 m) and scales (window sizes) by using imageries from Pléiades 1A, RapidEye, and Landsat-8 acquired in April 2013, the pre-monsoon season. Rao's Q index explained diversity more accurately than Shannon index for the three analyzed stand densities. Diversity was better approximated by Rao's Q index calculated by Pléiades 1A at a resolution of 0.5 m at low stand density. We observed higher correlations of the average coefficient of variation (CV) with Rao's Q and Shannon indices for areas associated with mixed spectral reflectance caused by overstory and understory vegetation. Furthermore, CV was lower in open areas dominated by lantana. These results indicated a strong scale and spatial resolution dependence of Rao's Q index on remote sensing-derived spectral heterogeneity information. When applied in heterogeneous forest environments, Rao's Q index could represent a better remote sensing proxy to estimate beta-diversity than the conventional Shannon index.

## 1. Introduction

Rapid industrialization and other anthropogenic factors during the last centuries caused dramatic changes to natural vegetation ecosystems. As a result, ecosystem components, such as plant biodiversity, have been experiencing a constant decline. This has been further exacerbated by the lack of knowledge on the biodiversity of large and remote ecosystems, which are generally inaccessible. Common challenges related to plant biodiversity include conducting regular inventories to quantify location and magnitude of biodiversity-related dynamics. It is now urgent to link these dynamics with human land use to monitor and sustain biodiversity (Bonanomi et al., 2018; Nagendra et al., 2010; Pettorelli et al., 2014a,b).

Although terrestrial measurements for large-area biodiversity assessments are the most accurate procedures for data collection and evaluation, large-scale field data collection is a challenge on a temporal

basis due to its requirement for extensive sampling (Gillespie et al., 2008; Hernández-Stefanoni et al., 2012; Palmer et al., 2002; Rocchini et al., 2005). Moreover, access to some regions is prevented due to climatic, geographic or socio-political reasons (Hanson et al., 2009; Rocchini et al., 2015). In contrast to ground-based observations, remote sensing data and methods offer cost-effective spatial solutions for biodiversity assessment of large or remote areas. Recent studies reported the usefulness of satellite remote sensing-based observations for modeling and assessment of essential biodiversity variables in order to plan conservation and management strategies (Kissling et al., 2018; Vihervaara et al., 2017).

Traditionally,  $\alpha$ - and  $\beta$ -diversities have been used for the assessment of biodiversity at local and regional scales, while their combination (termed  $\gamma$ -diversity) has been applied to estimate the entire diversity of a given area (Lande, 1996; Whittaker, 1972). Previous studies suggested remote sensing methods to estimate species

\* Corresponding author at: Department of Photogrammetry and Remote Sensing, Faculty of Geodesy and Geomatics Engineering, K. N. Toosi University of Technology, Tehran, Iran.

E-mail address: [hooman.latifi@kntu.ac.ir](mailto:hooman.latifi@kntu.ac.ir) (H. Latifi).

<https://doi.org/10.1016/j.ecolind.2019.105520>

Received 1 April 2019; Received in revised form 11 June 2019; Accepted 25 June 2019

Available online 28 June 2019

1470-160X/ © 2019 Elsevier Ltd. All rights reserved.

diversity (Levin et al., 2007; Oldeland et al., 2010; Rocchini et al., 2010; Wang et al., 2018, 2016b). Although all these studies primarily focused on the relationships between sample plot-based spectral values and  $\alpha$ -diversity (species diversity), others focused on the spectral rarefaction function relying on beta-diversity, i.e. between-plot spectral differences instead of between-plot species dissimilarities (Rocchini et al., 2011, 2009). Beta-diversity is defined as the proportion of turnover (spatial variation) in species abundance and composition from one site to another (Whittaker, 1972). Beta-diversity detects the relative abundance of different species along with species richness and the functional gradients determining the spatial variation in species composition (Rocchini, 2007). During the last decade, a few studies have explored new possibilities for remote sensing-based beta-diversity analysis by using the spectral heterogeneity information derived from image digital numbers at plot level (Hernández-Stefanoni et al., 2012; Rocchini et al., 2009, 2017).

The potential of spectral heterogeneity as a proxy for the analysis of species diversity (Rocchini et al., 2016, 2013) has recently been tested for plant species invading forests of the western Himalaya (Khare et al., 2018). The concept was extended to perform full remote sensing-based analysis to assess the spectral heterogeneity in large and mountainous reserved forest areas of Doon valley (Khare et al., 2018), where field data collection is not feasible on a temporal basis. This demonstrated the feasibility and tradeoffs of applying temporal multi-spatial resolution (at 30, 5 and 0.5 m) Landsat-8 OLI, RapidEye and Pléiades 1A datasets for species diversity analysis by deriving traditional Shannon entropy (Shannon, 1948) and Rényi (1970) indices.

A new index applied on remotely sensed data, Rao's Q, was suggested to overcome the numerical drawback of Shannon and Rényi diversity indices (Rocchini et al., 2018, 2017). Shannon index measures the richness and relative abundance of spectral values, yet it does not take into account the numerical magnitude of pixel values. On the contrary, Rao's Q index takes both numerical magnitude and pairwise distance of pixel values into account. Moreover, Shannon index relies solely on the relative proportion of digital numbers and is usually calculated on one single band at a time, whereas Rao's Q index allows multiple image bands to be considered simultaneously by building a distance matrix in several layers, maintaining its suitability for a multidimensional system (Rocchini et al., 2017).

In this study, we aim to extend the concept of remote sensing based assessment of beta-diversity using Rao's Q two dimensional space diversity. We compared the performance of the new Rao's Q with the conventional Shannon index for predicting species diversity at different spatial resolutions and scales (window sizes). We tested the new method for multi-scale assessment of species diversity using Landsat-8, RapidEye and Pléiades 1A optical datasets during the pre-monsoon season. Several studies have attempted to assess the field-based biodiversity of areas affected by the invasive lantana (*Lantana camara* L.) using the traditional Shannon index (Mandal and Joshi, 2015a, 2015b, 2014), while some attempted remote sensing-based mapping and identification of lantana-occupied sites (Gairola et al., 2013; Kimothi and Dasari, 2010). However, to our knowledge, this is the first study to estimate beta-diversity using high spatial resolution satellite remote sensing derived Rao's Q index in remote reserved forests affected by lantana invasion. We expected that these data would be suitable proxies for species diversity analysis.

## 2. Materials and methods

### 2.1. Study area

The study area is located in the Western Himalayan region of Doon valley, Uttarakhand, India (29°55' to 30°30' N and 77°35' to 78°24'E), at elevations ranging between 500 and 800 m above sea level (Fig. 1). The Lachhiwala forest within the study area was selected due to its wide variability in canopy coverage and topography. The climate is humid

sub-tropical, with temperatures ranging from 16 to 36 °C in summer and 5 to 23 °C in winter (Peel et al., 2007). Annual rainfall is 2025 mm that is mainly concentrated between June and September. The vegetation is subtropical moist deciduous forest, dominated by *Shorea robusta* (Sal tree) in the overstory, with other species such as *Mallotus philippensis* Lam., *Clerodendrum infortunatum* L. and lantana in the understorey.

### 2.2. Satellite and field data

We used two cloud-free and orthorectified images acquired in April 2013, the pre-monsoon season: the Pléiades 1A image (5 April) with four spectral bands and spatial resolution of 0.5 m, and Level 3A RapidEye image (12 April) with five spectral bands and spatial resolution of 5 m.

RapidEye sensor features an additional red-edge band with spectral range of 690–730 nm (specifications are given in Chander et al., 2013). The Level 3A product already includes radiometric and geometric corrections. Atmospheric corrections were subsequently performed to convert DN values into surface reflectance using ATCOR 3 (Richter, 2007). Normalized Difference Vegetation Indices (NDVI) were generated from surface reflectance values (Rouse et al., 1974). Preprocessed Landsat-8 OLI data were acquired from USGS (United States Geological Survey) for April 2013. We selected Blue, Green, Red and near infrared (NIR) bands of Landsat-8 OLI data to match the spectral ranges of RapidEye and Pléiades 1A multispectral imagery.

Field data were collected during April 2013 to identify the lantana-occupied locations using Global Positioning System (GPS) points within the selected site named b in Fig. 1 (Khare et al., 2018). Because of its protection within the reserve, and difficult accessibility, data collection was permitted only at the border of the forest. Sample plots 1, 4 and 5 in site (b) include Sal trees with some canopy gaps and shadows. Plots 2, 3 and 6 have open areas with clearly visible lantana dominance (Fig. 1).

### 2.3. Remote sensing-based estimation of diversity

Three sites were identified according to stand density: (a) Low Density Forest (LDF), (b) Medium Density Forest (MDF), and (c) High Density Forest (HDF) (Fig. 1). April is the dry season, when shedding of *S. robusta* leaves is maximum (Khare et al., 2018, 2017). The presence of understorey shrub species is therefore evident in LDF. The understorey shrubs in MDF contribute to overall spectral reflectance due to shedding of leaves by the overstorey vegetation. The visibility of understorey shrubs in HDF cover is negligible due to high density of the overstorey.

NDVI, a proxy of vegetation photosynthetic activity, is a vegetation index to predict species richness and diversity (Arekhi et al., 2017; He et al., 2009) represented by the ratio  $(\lambda_{\text{NIR}} - \lambda_{\text{R}})/(\lambda_{\text{NIR}} + \lambda_{\text{R}})$ , where  $\lambda_{\text{NIR}}$  and  $\lambda_{\text{R}}$  are the reflectance of red and NIR bands, respectively (Lillesand et al., 2004). NDVI is considered as a valid indicator to relate species diversity with variations in tree or plant leaf spectral reflectance observed in red and NIR electromagnetic spectrum ranges (Arekhi et al., 2017; Rocchini et al., 2009). In each site, the NDVI was calculated for Landsat-8, RapidEye and Pléiades 1A datasets at spatial resolutions of 30 m, 5 m and 0.5 m, and diversity indices were estimated using Rao's Q and Shannon indices at two window sizes ( $3 \times 3$  and  $9 \times 9$  pixels). We used the routine initially developed by Rocchini et al. (2017) in R open source domain (R Core Team, 2016). The mathematical description of Rao's Q index is available in the supplementary material (SFig. 1) as well as in Rocchini et al. (2017).

#### 2.3.1. Modeling NDVI with Rao's Q and Shannon

We performed linear regression models to evaluate the relationships between NDVI and Rao's Q and Shannon indices according to previous studies (Wang et al., 2016b). We modeled the Rao's Q ( $Q_3$ ,  $Q_9$ ) and Shannon ( $H_3$ ,  $H_9$ ) diversity spectral metrics with their corresponding

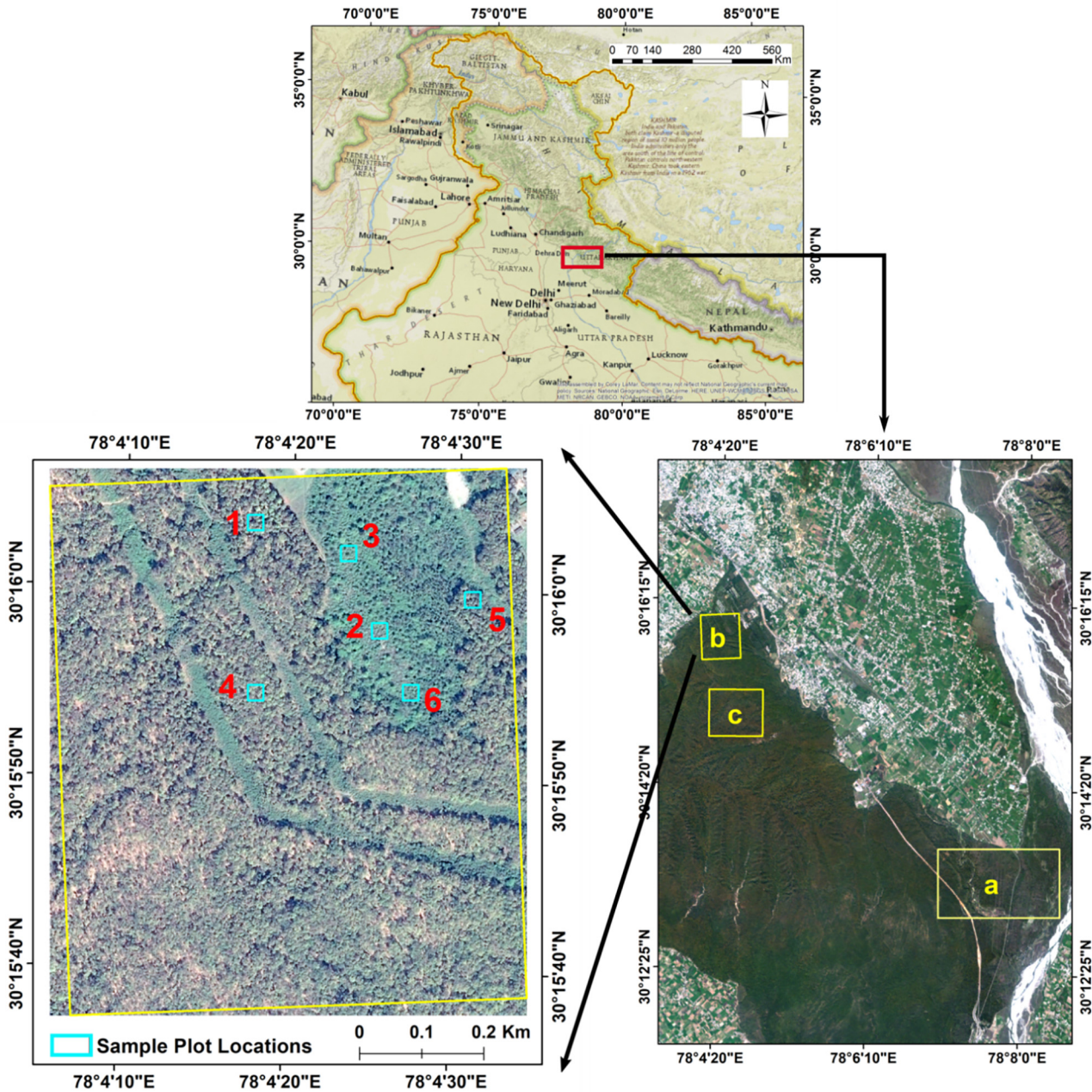


Fig. 1. Locations of study sites (a) LDF (b) MDF and (c) HDF depicted on RapidEye True Color Composite (TCC) imagery. Zoomed location within study site LDF shows the six field based-sample plots.

NDVI spectral metrics derived at different spatial resolution for each window size.

2.3.2. Plot level measurement of coefficient of variation

As an indicator of spectral diversity, we used average coefficient of variation (CV) (Wang et al., 2018, 2016a), which is calculated as the average of CV for each spectral wavelength of Blue, Green, Red and NIR bands (430–950 nm) for the four multispectral bands of Pléiades 1A and Landsat-8, and five multispectral bands of RapidEye.

$$CV_{plot_n} = \frac{\sum_{\lambda=430}^{950} \left( \frac{\sigma(\rho_{\lambda})}{\mu(\rho_{\lambda})} \right)}{\text{number of multispectral bands}} \quad (1)$$

where  $\rho_{\lambda}$  represents the wavelength ( $\lambda$ ) and  $\sigma(\rho_{\lambda})$ ,  $\mu(\rho_{\lambda})$  denotes the standard deviation and mean value at wavelength ( $\lambda$ ) across all the pixels in  $plot_n$ , where n denotes the sample plot number.

We used a chessboard segmentation method (Baatz et al., 2004) that enabled a flawless matching of the image-derived parameters with the field-based locations marked for lantana invaded areas with the help of GPS (Khare et al., 2018). In this method, a given image is split into square image objects of the same size. The object size was set to  $10 \times 10$  m sample plots, corresponding to  $20 \times 20$  pixels in Pléiades 1A imagery (Fig. 1). We extracted the  $CV_{plot_n}$  and Rao's Q diversity values for each square image object of sample plot locations and then calculated the correlation between them. These image-derived values for each square object correspond to the field-based locations calculated for each sample plot.

3. Results

Pléiades 1A, RapidEye and Landsat-8 enabled to reveal significant ( $p < 0.001$ ) relationships between Rao's Q and NDVI for all three

**Table 1**

Rao's Q and Shannon's H diversity-NDVI modeled relationships. Values shown are multiple linear regression parameters, including model equation, and F value. Significant codes: 0.05 < p, \*, 0.05 < p < 0.01, \*\*, 0.001 < p < 0.01 and \*\*\*, p < 0.001.

Forest Density	Satellite Data	F value – Rao's Q		F value – Shannon	
		3 × 3 (pixels)	9 × 9 (pixels)	3 × 3 (pixels)	9 × 9 (pixels)
LDF	Landsat-8	47.03***	8.46**	2.33	2.55
	RapidEye	28.42***	0.18	4.51*	111.53***
	Pléiades 1A	88.23***	52.79***	30.92***	9.18**
MDF	Landsat-8	20.13***	10.81**	9.84**	0.49
	RapidEye	31.77***	25.37***	6.2*	11.13**
	Pléiades 1A	50.97***	38.81***	3.67*	0.479
HDF	Landsat-8	26.65***	0.06	2.31	3.57
	RapidEye	0.74	0.39	0.04	2.39
	Pléiades 1A	28.02***	26.31***	26.29***	24.81***

forest density categories at a scale of 3 × 3 (Table 1). The strongest relationships were obtained for Pléiades 1A (0.5 m) when compared to RapidEye (5 m) and Landsat-8 (30 m) at both scales for each forest density category (Table 1). Moreover, RapidEye and Landsat-8 were not able to explain the Rao's Q and NDVI relationship, and were not significant for HDF (Table 1).

The relationship between Shannon and NDVI in the case of RapidEye was weak for LDF and MDF at scale 3 × 3 (p < 0.05) when compared with a scale of 9 × 9 (for LDF p < 0.001 and for MDF p < 0.01) (Table 1). However, it was significant in the case of Landsat-8 for MDF at scale 3 × 3. RapidEye and Landsat-8 results were not able to explain the Shannon and NDVI relationship and were not significant for HDF (Table 1). Instead, Pléiades 1A data provided the strongest relationship at scale 3 × 3 (p < 0.001) compared to scale 9 × 9 for LDF and HDF, while the relationship was weak (p < 0.05) for MDF at scale 3 × 3.

The understory vegetation was clearly visible in LDF, especially with RapidEye and Pléiades 1A (Fig. 2). MDF included spectral reflectance of both overstory and understory vegetation due to shedding of overstory vegetation leaves (Fig. 3). At 0.5 m spatial resolution, the NDVI was not hampered by mixed pixels problem compared to 30 and 5 m, so results enabled to provide an effective Rao's Q-NDVI relationship for Pléiades 1A. Only overstory vegetation was visible on HDF (Fig. 4), hence there was a minimal contribution of spectral reflectance from understory vegetation. Therefore, understory greenness

was not visible at spatial resolutions of 30 and 5 m (Fig. 4). Some shedding of leaves by the overstory vegetation was, however, visible due to the dry season, allowing a degree of spectral reflectance of the understory vegetation to be detected at 0.5 m spatial resolution. Consequently, we observed a minor difference in Rao's-NDVI and Shannon's H-NDVI relationship at 0.5 m spatial resolution for Pléiades 1A data (Table 1). For both window sizes, Rao's Q significantly described gradients of spatial diversity compared to Shannon in LDF and MDF categories, which show high spatial heterogeneity with the presence of larger trees and shrubs (Figs. 3 and 4).

RapidEye and Pléiades 1A-based Rao's Q indices enabled approximating the variation of species diversity for both 3 × 3 and 9 × 9 window sizes (Table 2, Fig. 5). The CV values for plots 1, 4, 5 were 15.8, 13.05, 22.92 in the case of RapidEye, whereas they were 22.64, 19.29, 22.44 respectively for Pléiades 1A. Similarly, values for plots 2, 3, 6 were 0.3, 12.08, 10.38 for RapidEye and 13.78, 15.54, 15.13 for Pléiades 1A, respectively (Table 2). Moreover, CV was higher for Pléiades 1A for plots 1, 4 and 5, which represented combinations of Sal trees with some canopy gaps and understory lantana when compared to RapidEye and Landsat-8 (Table 2, Fig. 5). CV was lower at all spatial resolutions for plots 2, 3 and 6, which mainly consisted of a single plant species (lantana) established in an open area (Fig. 5), and clearly showed low spatial resolution data encountered with mixed pixel problems in areas of higher species diversity. Results indicated that the Shannon index provided higher mean values than Rao's Q index for each sample plot, which suggested its tendency to overestimate species diversity.

The variation in spectral resolution was investigated using the average CV. Compared to spatial resolutions of 5 m (RapidEye), the average CV was higher at spatial resolutions of 1.5 m (Pléiades 1A) due to a more detailed visibility of over- and understory vegetation (Fig. 5). The mean values of Rao's Q and Shannon indices were higher for RapidEye when compared to Pléiades 1A for the six plots and two window sizes (Table 2). This result was explained by the fact that RapidEye records spectral information in 5 different wavelength regions (4 visible and 1 NIR bands), whereas Pléiades 1A records in 4 wavelength regions (3 visible and 1 NIR).

**4. Discussion**

**4.1. Observed beta-diversity by remote sensing**

In this study, we extended the concept of a fully remote sensing-based approach to measure beta-diversity using Rao's Q at multiple

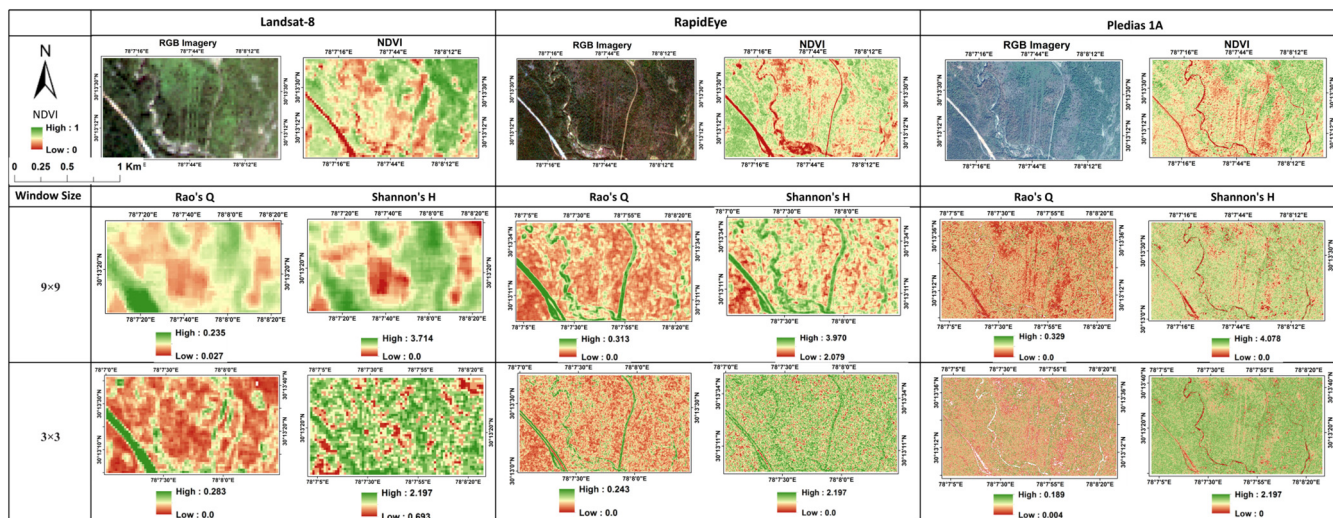


**Fig. 2.** Rao's Q and Shannon's H diversity maps for LDF category.

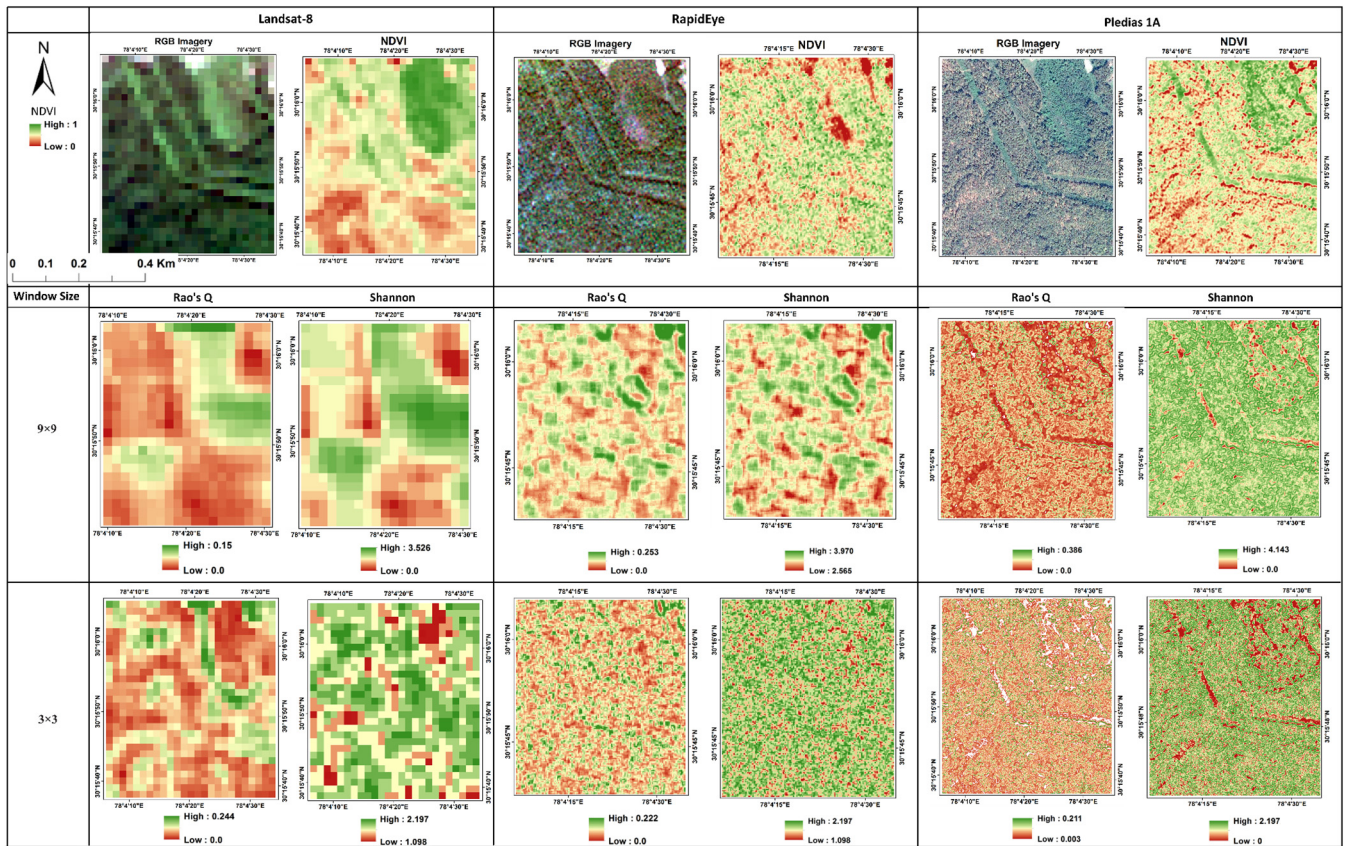


Fig. 3. Rao's Q and Shannon's H diversity maps for MDF category.

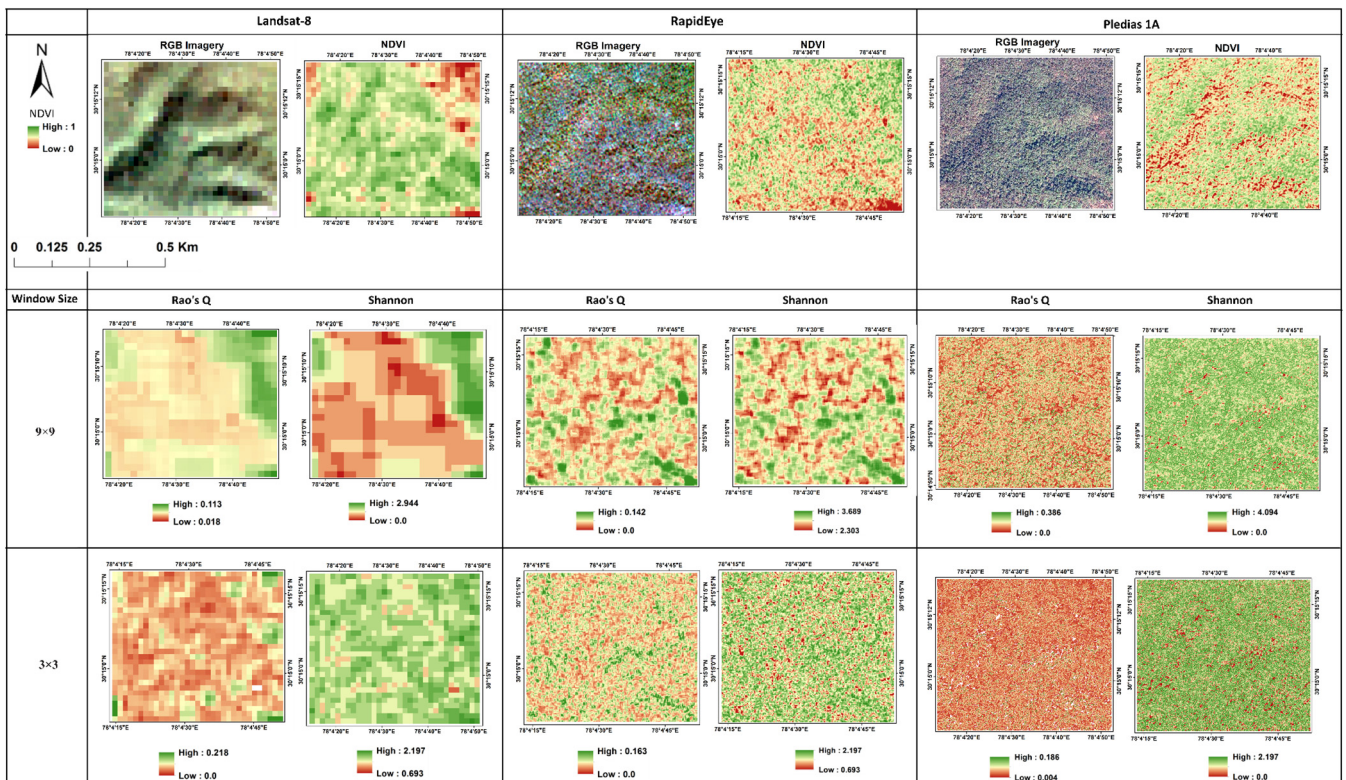


Fig. 4. Rao's Q and Shannon's H diversity maps for HDF category.

**Table 2**  
Plot-wise statistical computation of Rao's Q and Shannon's H indices for scales  $3 \times 3$  and  $9 \times 9$  pixels.

Satellite Data	Plot	CV	Rao's Q		Shannon	
			$3 \times 3$ (pixels)	$9 \times 9$ (pixels)	$3 \times 3$ (pixels)	$9 \times 9$ (pixels)
Landsat-8	1	6.22	0.028	0.115	1.767	3.310
	3	4.00	0.031	0.106	1.445	3.135
	5	9.38	0.033	NA	1.830	NA
	2	4.65	0.019	0.091	1.609	3.219
	4	4.76	0.027	0.065	1.739	2.993
	6	4.31	0.036	0.112	1.785	3.401
RapidEye	1	15.80	0.048	0.081	1.999	3.222
	3	12.08	0.032	0.080	1.786	3.177
	5	22.92	0.065	0.113	2.059	3.493
	2	10.30	0.053	0.121	2.020	3.508
	4	13.05	0.055	0.092	1.862	3.259
	6	10.38	0.044	0.099	1.975	3.398
Pléiades 1A	1	22.64	0.035	0.101	1.555	2.938
	3	15.54	0.016	0.038	1.080	2.227
	5	22.44	0.035	0.103	1.576	2.949
	2	13.78	0.025	0.070	1.426	2.697
	4	19.29	0.034	0.101	1.593	2.960
	6	15.13	0.018	0.047	1.160	2.359

spatial resolutions (30, 5 and 0.5 m) and scales ( $3 \times 3$  and  $9 \times 9$ ) of remote sensing datasets, and compared the results with the Shannon index in three different forest density classes. The study was initially promoted by the basic concept suggested by Khare et al. (2018), deriving remote sensing based Rényi and Shannon indices to assess species diversity in areas colonized by lantana. We adopted and extended the concept on the optical remote sensing-based assessment of beta-diversity by means of Rao's Q index (Rocchini et al., 2017).

#### 4.2. Performance comparison of Rao's Q and Shannon indices

A recent study compared the performance of Rao's Q and Shannon indices at a spatial resolution of 10 m (Sentinel-2A imagery) using window size  $3 \times 3$  (Rocchini et al., 2018). Our results are in agreement with this study, which showed that Rao's diversity measured the magnitude of two pixels along with their pairwise distance. Results from Rao's Q index were therefore more significant for all the datasets when compared to Shannon-based outputs. These findings suggest that the Shannon index (as the most commonly applied diversity index) tends to overestimate the diversity because it considers the proportion of two pixel values instead of their magnitudes.

Across the three forest density covers analyzed in our study, the conventional Shannon index overestimated species diversity at varying spatial resolution when compared to Rao's Q index, which complemented the previous study of Rocchini et al. (2018). In addition, our results demonstrated that estimation of beta-diversity using Rao's Q diversity for heterogeneous environments (LDF and MDF covers in our case) was more significant when compared to the Shannon index, which also agreed with previous studies (Feilhauer and Schmidlein, 2009; Hernández-Stefanoni et al., 2012; Rocchini et al., 2014). Moreover, both indices were saturated in the case of homogenous, dense forest stands (HDF category) at all spatial resolutions, since only the top of overstory vegetation was visible. This was in agreement with a previous study in which both Rényi and Shannon indices were infeasible to explain the diversity for high density forest covers (Khare et al., 2018). However, in this study, Rao's Q index outperformed the Shannon index. This is presumably related to the continuous diversity trend of Rényi and Shannon indices, which only consider the relative proportion of spectral values. On the contrary, Rao's Q index takes the pairwise distances between pixel values into account besides their relative proportion (Rocchini et al., 2017).

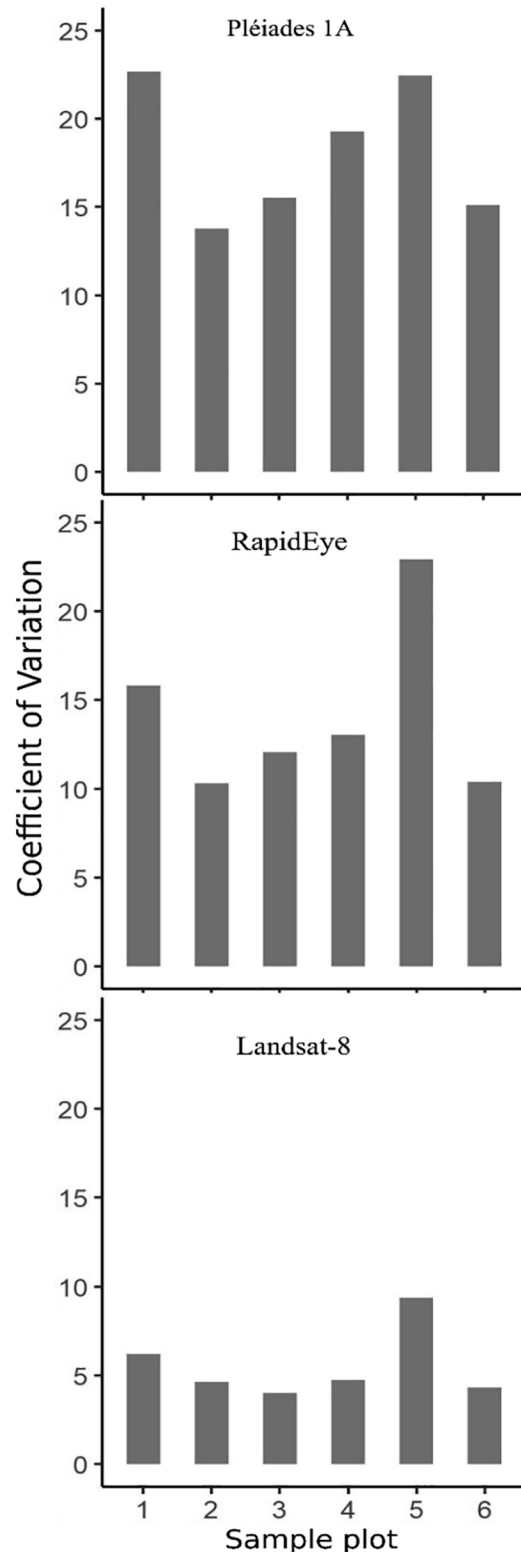


Fig. 5. Plot-level combined scores of CV and Rao's Q index for Landsat-8, RapidEye and Pléiades 1A for window size  $3 \times 3$ .

Our results suggest that medium and high spatial resolution remote sensing based biodiversity analyses are more appropriate for investigations of heterogeneous environments. In addition, this study utilized the potential of NDVI and our results agreed with previous studies (Feilhauer et al., 2012; He et al., 2009; Hernández-Stefanoni et al., 2012; Khare et al., 2016; Wang et al., 2016a,b) which also used

NDVI as a remote sensing index for biodiversity analysis. Our results also suggested that high spatial resolution-based NDVI was more suitable to explain the spectral heterogeneity, especially in small areas where understory vegetation is more dominant. However, high spatial resolution multispectral remote sensing datasets may exhibit limitations for performing temporal biodiversity analyses on larger areas due to their high cost. In this case, open access multispectral Sentinel-2A, 2B and Landsat archives may be used as an alternative for long-term temporal analyses.

#### 4.3. Scale, spatial and spectral resolution dependence of species diversity

We used the average coefficient of variation (CV) of spectral reflectance as an indicator of spectral diversity, which was then compared against both the new Rao's Q and the conventional Shannon index. There are only a few previous published studies on the topic (Khare et al., 2018; Wang et al., 2018), with which our results agreed in showing that forest patches (here sample plots) with higher CVs were associated with higher species diversities. However, an older study by Lucas and Carter (2008) reported negative relationship between CV and species diversity due to mixed spectral reflectance of soil background and vegetation within in Horn Island, Mississippi, USA.

In remote sensing, the pixel size (spatial resolution) related to the spatial structure of the size of the object on the earth surface and local variance increased when size of the object size is close to the spatial resolution of the imagery (Woodcock and Strahler, 1987; Wang et al., 2018). In another study, the Shannon index was well correlated with corresponding sample plots CV computed from 1.1 m spatial resolution airborne imagery of prairie grassland in southern Alberta, Canada (Wang et al., 2016b). Our results were in accordance with these previous studies, which revealed that species diversity was better explained at a higher spatial resolution (0.5 m pixel size).

Previous papers reported that an inappropriate match of field-based grain size and remote sensing-based spatial resolution may hamper relating the measured spatial heterogeneity with sub-pixel level variability (Rocchini, 2007; Small, 2004), which was in line with our multi-scale, multi-spatial resolution observations. Our study revealed that the difference in CV between diversity levels increased along with the increase in spatial resolution, which, in turn, greatly increased the ability to optically detect biodiversity. Since the smaller scale ( $3 \times 3$ ) covers fewer species than the bigger scale ( $9 \times 9$ ), the values of Rao's Q and Shannon indices were higher for the bigger scale (Table 2) for all the remote sensing datasets. Thus, our results also suggested that higher spatial resolutions and smaller window size filters provide the closest approximations of species diversity expressed as spatial heterogeneity. In addition, a previous study (Foody, 2004) reported that correlation between spectral variability and species diversity increased with multi-scale analysis. Our results also suggested that diversity-NDVI relationship could be sensitive to the scale and spatial resolution used. Future studies should involve other multispectral remote sensing based vegetation indices-diversity relationships, including red-edge bands due to their ability to record differences in leaf structure and chlorophyll content. For instance, red-edge based NDRE (normalized difference red-edge) index (Viña and Gitelson, 2005) could be tested for RapidEye (Schuster et al., 2012) and Sentinel-2A, 2B (Delegido et al., 2011) satellite data.

Spectral resolution also plays an important role in understanding landscape diversity. It resulted in an increase in accuracy of diversity estimation by adding additional spectral wavelengths (Rocchini, 2007). In our case, with RapidEye (including spectra of red-edge band) overall Rao's Q mean values of all the sample plots were higher when compared to Pléiades 1A. This indicated that spectral resolution is also an essential parameter along with spatial resolution for biodiversity estimation. This type of analysis is worth testing for freely-available Sentinel-2A, 2B data which include three vegetation red-edge and two near infrared (NIR and narrow NIR) bands with varying spatial resolutions.

## 5. Conclusion

In this study, we estimated beta-diversity using multi-scale, multi-resolution remote sensing data and compared Rao's Q and Shannon index for a remote forest area where species inventory field data collection is not possible. Indeed, field observation was limited to verifying the presence and location of lantana at the border of the reserved forest. When compared with the Shannon index, Rao's Q index was able to explain diversity more accurately at multi-spatial resolutions and scales. The Shannon index overestimated diversity because it considers only the proportion of two pixel values instead of their magnitudes, whereas Rao's Q index involves both magnitude and pairwise distance of pixels. We demonstrated that the estimated diversity increased with scale sizes. We observed that the best spatial resolution to estimate beta-diversity using spectral diversity indicator (average CV) was 0.5 m, when compared with 5 and 30 m. The observed spectral heterogeneity especially in heterogeneous forest areas was successfully explained by the distance and abundance-based method of Rao's Q index at spatial resolutions of 0.5 and 5 m compared to 30 m. Lower resolution (30 m) data recorded less spatial complexity and spectral heterogeneity due to mixed pixel problems. The beta-diversity estimation using Rao's Q index was most effective in open areas with visible understory vegetation, where optical satellite imagery recorded unhampered spectral signatures.

## Acknowledgements

We thank U.S. Geological Survey (USGS) EROS data center, RapidEye Science Archive (RESA) and European Space Agency (ESA) for providing remote sensing datasets, and A. Garside for checking the English text.

## Funding

ESA with project id: 33429 for providing Pléiades 1A dataset; RESA with project id: 00184 for providing RapidEye datasets.

## Appendix A. Supplementary data

Supplementary data to this article can be found online at <https://doi.org/10.1016/j.ecolind.2019.105520>.

## References

- Arekhi, M., Yılmaz, O.Y., Yılmaz, H., Akyüz, Y.F., 2017. Can tree species diversity be assessed with Landsat data in a temperate forest? *Environ. Monit. Assess.* 189 (11), 586. <https://doi.org/10.1007/s10661-017-6295-6>.
- Baatz, M., Benz, U., Deghani, S., Heynen, M., Hölzle, A., Hofmann, P., Lingenfelder, I., Mimler, M., Sohlbach, M., Weber, M., Willhauck, G., 2004. eCognition User Guide. Definiens Imaging GmbH, Munich, Germany.
- Bononomi, G., Allevato, E., Rita, A., Cesarano, G., Saulino, L., Di Pasquale, G., Allegranza, M., Pesaresi, S., Borghetti, M., Rossi, S., Saracino, A., 2018. Anthropogenic and environmental factors affect the tree line position of *Fagus sylvatica* along the Apennines (Italy). *J. Biogeogr.* 45, 2595–2608. <https://doi.org/10.1111/jbi.13408>.
- Chander, G., Haque, M.O., Sampath, A., Brunn, A., Trosset, G., Hoffmann, D., Roloff, S., Thiele, M., Anderson, C., 2013. Radiometric and geometric assessment of data from the RapidEye constellation of satellites. *Int. J. Remote Sens.* 34, 5905–5925. <https://doi.org/10.1080/01431161.2013.798877>.
- Delegido, J., Verrelst, J., Alonso, L., Moreno, J., 2011. Evaluation of sentinel-2 red-edge bands for empirical estimation of green LAI and chlorophyll content. *Sensors* 11, 7063–7081. <https://doi.org/10.3390/s110707063>.
- Feilhauer, H., He, K.S., Rocchini, D., 2012. Modeling species distribution using niche-based proxies derived from composite bioclimatic variables and MODIS NDVI. *Remote Sens.* 4, 2057–2075. <https://doi.org/10.3390/rs4072057>.
- Feilhauer, H., Schmidtlein, S., 2009. Mapping continuous fields of forest alpha and beta diversity. *Appl. Veg. Sci.* 12, 429–439. <https://doi.org/10.1111/j.1654-109X.2009.01037.x>.
- Foody, G.M., 2004. Spatial nonstationarity and scale-dependency in the relationship between species richness and environmental determinants for the sub-Saharan endemic avifauna. *Glob. Ecol. Biogeogr.* 13, 315–320.
- Gairola, S., Procheş, Ş., Rocchini, D., 2013. High-resolution satellite remote sensing: a new frontier for biodiversity exploration in Indian Himalayan forests. *Int. J. Remote*

- Sens. 34, 2006–2022. <https://doi.org/10.1080/01431161.2012.730161>.
- Gillespie, T.W., Foody, G.M., Rocchini, D., Giorgi, A.P., Saatchi, S., 2008. Measuring and modelling biodiversity from space. *Prog. Phys. Geogr.* 32 (2), 203–221. <https://doi.org/10.1177/0309133308093606>.
- Hanson, T., Brooks, T.M., Da Fonseca, G.A.B., Hoffmann, M., Lamoreux, J.F., Machlis, G., Mittermeier, R.A., Mittermeier, C.G., Pilgrim, J.D., 2009. Warfare in biodiversity hotspots. *Conserv. Biol.* 23, 578–587. <https://doi.org/10.1111/j.1523-1739.2009.01166.x>.
- He, K.S., Zhang, J., Zhang, Q., 2009. Linking variability in species composition and MODIS NDVI based on beta diversity measurements. *Acta Oecologica* 35, 14–21. <https://doi.org/10.1016/j.actao.2008.07.006>.
- Hernández-Stefanoni, J.L., Gallardo-Cruz, J.A., Meave, J.A., Rocchini, D., Bello-Pineda, J., López-Martínez, J.O., 2012. Modeling  $\alpha$ - and  $\beta$ -diversity in a tropical forest from remotely sensed and spatial data. *Int. J. Appl. Earth Obs. Geoinf.* 19, 359–368. <https://doi.org/10.1016/j.jag.2012.04.002>.
- Khare, S., Ghosh, S.K., Latifi, H., Vijay, S., Dahms, T., 2017. Seasonal-based analysis of vegetation response to environmental variables in the mountainous forests of western Himalaya using Landsat 8 data. *Int. J. Remote Sens.* 38 (15), 4418–4442. <https://doi.org/10.1080/01431161.2017.1320450>.
- Khare, S., Latifi, H., Ghosh, S.K., 2018. Multi-scale assessment of invasive plant species diversity using Pléiades 1A, RapidEye and Landsat-8 data. *Geocarto Int.* 33 (7), 681–698. <https://doi.org/10.1080/10106049.2017.1289562>.
- Khare, S., Latifi, H., Ghosha, K., 2016. Phenology analysis of forest vegetation to environmental variables during pre- and post-monsoon seasons in western Himalayan region of India, in: *International Archives of the Photogrammetry, Remote Sensing and Spatial Information Sciences – ISPRS Archives*. <https://doi.org/10.5194/isprsarchives-XLI-B2-15-2016>.
- Kimothi, M.M., Dasari, A., 2010. Methodology to map the spread of an invasive plant (Lantana camara L.) in forest ecosystems using Indian remote sensing satellite data. *Int. J. Remote Sens.* 31, 3273–3289. <https://doi.org/10.1080/014311690903121126>.
- Kissling, W.D., Ahumada, J.A., Bowser, A., Fernandez, M., Fernández, N., García, E.A., Guralnick, R.P., Isaac, N.J.B., Kelling, S., Los, W., McRae, L., Mihoub, J.B., Obst, M., Santamaria, M., Skidmore, A.K., Williams, K.J., Agosti, D., Amariles, D., Arvanitidis, C., Bastin, L., De Leo, F., Egloff, W., Elith, J., Hobern, D., Martin, D., Pereira, H.M., Pesole, G., Peterseil, J., Saarenmaa, H., Schigel, D., Schmeller, D.S., Segata, N., Turak, E., Uhlir, P.F., Wee, B., Hardisty, A.R., 2018. Building essential biodiversity variables (EBVs) of species distribution and abundance at a global scale. *Biol. Rev.* 93, 600–625. <https://doi.org/10.1111/brv.12359>.
- Lande, R., 1996. Statistics and partitioning of species diversity, and similarity among multiple communities. *Oikos* 76, 5–13.
- Levin, N., Shmida, A., Levanoni, O., Tamari, H., Kark, S., 2007. Predicting mountain plant richness and rarity from space using satellite-derived vegetation indices. *Divers. Distrib.* 13, 692–703. <https://doi.org/10.1111/j.1472-4642.2007.00372.x>.
- Lillesand, T.M., Kiefer, R.W., Chipman, J.W., 2004. *Remote Sensing and Image Interpretation*, 5th ed. John Wiley & Sons, New York, USA.
- Lucas, K.L., Gregory, A.C., 2008. The use of hyperspectral remote sensing to assess vascular plant species richness on Horn Island, Mississippi. *Remote Sens. Environ.* 112 (10), 3908–3915. <https://doi.org/10.1016/j.rse.2008.06.009>.
- Mandal, G., Joshi, S.P., 2015a. Plant invasion: dynamics and habitat invasion capacity of invasive species in Western Indian Himalaya. *Ann. di Bot.* 5, 1–16. <https://doi.org/10.4462/annbotm-12469>.
- Mandal, G., Joshi, S.P., 2015b. Eco-physiology and habitat invisibility of an invasive, tropical shrub (Lantana camara) in western Himalayan forests of India. *Forest Sci. Technol.* 0103, 37–41. <https://doi.org/10.1080/21580103.2014.990062>.
- Mandal, G., Joshi, S.P., 2014. Analysis of vegetation dynamics and phytodiversity from three dry deciduous forests of Doon Valley, Western Himalaya, India. *J. Asia-Pacific Biodivers.* 7, 292–304. <https://doi.org/10.1016/j.japb.2014.07.006>.
- Nagendra, H., Rocchini, D., Ghate, R., Sharma, B., Pareeth, S., 2010. Assessing plant diversity in a dry tropical forest: comparing the utility of Landsat and Ikonos satellite images. *Remote Sens.* 2, 478–496. <https://doi.org/10.3390/rs2020478>.
- Oldeland, J., Wesuls, D., Rocchini, D., Schmidt, M., Jürgens, N., 2010. Does using species abundance data improve estimates of species diversity from remotely sensed spectral heterogeneity? *Ecol. Indic.* 10, 390–396. <https://doi.org/10.1016/j.ecolind.2009.07.012>.
- Palmer, M.W., Earls, P.G., Hoagland, B.W., White, P.S., Wohlgemuth, T., 2002. Quantitative tools for perfecting species lists. *Environmetrics* 13, 121–137. <https://doi.org/10.1002/env.516>.
- Peel, M.C., Finlayson, B.L., McMahon, T.A., 2007. World map of the Köppen-Geiger climate classification updated. *Meteorol. Zeitschrift* 15, 259–263. <https://doi.org/10.1127/0941-2948/2006/0130>.
- Pettorelli, N., Laurance, W.F., O'Brien, T.G., Wegmann, M., Nagendra, H., Turner, W., 2014a. Satellite remote sensing for applied ecologists: opportunities and challenges. *J. Appl. Ecol.* 51, 839–848. <https://doi.org/10.1111/1365-2664.12261>.
- Pettorelli, N., Nagendra, H., Williams, R., Rocchini, D., Fleishman, E., 2014b. A new platform to support research at the interface of remote sensing, ecology and conservation. *Remote Sens. Ecol. Conserv.* 1, 1–3. <https://doi.org/10.1002/rse2.1>.
- R Core Team, 2016. R: A language and environment for statistical computing. R Foundation for Statistical Computing, Vienna, Austria. <http://www.R-project.org/>.
- Rényi, A., 1970. *Probability Theory*. North Holland Publishing Company, Amsterdam.
- Richter, R., 2007. Atmospheric/Topographic Correction for Satellite Imagery (ATCOR – 2/3 User Guide). ATCOR-2/3 User Guide Version 6.3 1–71. <https://doi.org/10.1017/CBO9781107415324.004>.
- Rocchini, D., 2007. Effects of spatial and spectral resolution in estimating ecosystem  $\alpha$ -diversity by satellite imagery. *Remote Sens. Environ.* 111 (4), 423–434. <https://doi.org/10.1016/j.rse.2007.03.018>.
- Rocchini, D., Balkenhol, N., Carter, G.A., Foody, G.M., Gillespie, T.W., He, K.S., Kark, S., Levin, N., Lucas, K., Luoto, M., Nagendra, H., Oldeland, J., Ricotta, C., Southworth, J., Neteler, M., 2010. Remotely sensed spectral heterogeneity as a proxy of species diversity: recent advances and open challenges. *Ecol. Inform.* 5, 318–329. <https://doi.org/10.1016/j.ecoinf.2010.06.001>.
- Rocchini, D., Dadalt, L., Delucchi, L., Neteler, M., Palmer, M.W., 2014. Disentangling the role of remotely sensed spectral heterogeneity as a proxy for North American plant species richness. *Community Ecol.* 15 (1), 37–43. <https://doi.org/10.1556/comec.15.2014.1.4>.
- Rocchini, D., Delucchi, L., Bacaro, G., 2016. The power of generalized entropy for biodiversity assessment by remote sensing: an open source approach. *Springer Proc. Math. Stat.* 227, 1–7.
- Rocchini, D., Delucchi, L., Bacaro, G., Cavallini, P., Feilhauer, H., Foody, G.M., He, K.S., Nagendra, H., Porta, C., Ricotta, C., Schmidlein, S., Spano, L.D., Wegmann, M., Neteler, M., 2013. Calculating landscape diversity with information-theory based indices: a GRASS GIS solution. *Ecol. Inform.* 17, 82–93. <https://doi.org/10.1016/j.ecoinf.2012.04.002>.
- Rocchini, D., Hernández-Stefanoni, J.L., He, K.S., 2015. Advancing species diversity estimate by remotely sensed proxies: a conceptual review. *Ecol. Inform.* 25, 22–28. <https://doi.org/10.1016/j.ecoinf.2014.10.006>.
- Rocchini, D., Luque, S., Pettorelli, N., Bastin, L., Doktor, D., Faedi, N., Feilhauer, H., Féret, J.-B., Foody, G.M., Gavish, Y., Godinho, S., Kunin, W.E., Lausch, A., Leitão, P.J., Marcantonio, M., Neteler, M., Ricotta, C., Schmidlein, S., Vihervaaara, P., Nagendra, H., 2018. Measuring  $\beta$ -diversity by remote sensing: a challenge for biodiversity monitoring. *Methods Ecol. Evol.* 9, 1787–1798. <https://doi.org/10.1111/2041-210x.12941>.
- Rocchini, D., Marcantonio, M., Ricotta, C., 2017. Measuring Rao's Q diversity index from remote sensing: an open source solution. *Ecol. Indic.* 72, 234–238. <https://doi.org/10.1016/j.ecolind.2016.07.039>.
- Rocchini, D., McGlenn, D., Ricotta, C., Neteler, M., Wohlgemuth, T., 2011. Landscape complexity and spatial scale influence the relationship between remotely sensed spectral diversity and survey-based plant species richness. *J. Veg. Sci.* 22, 688–698. <https://doi.org/10.1111/j.1654-1103.2010.01250.x>.
- Rocchini, D., Perry, G.L.W., Salerno, M., Maccherini, S., Chiarucci, A., 2005. Landscape change and the dynamics of open formations in a natural reserve. *Landscape Urban Plan.* 77, 167–177. <https://doi.org/10.1016/j.landurbplan.2005.02.008>.
- Rocchini, D., Wohlgemuth, T., Ricotta, C., Ghisleni, S., Stefanini, A., Chiarucci, A., 2009. Rarefaction theory applied to satellite imagery for relating spectral and species diversity. *Ital. di Telerilevamento* 41, 109–123. <https://doi.org/10.5721/IJRS20094128>.
- Rouse, W., Haas, H., Deering, W., 1974. 20 monitoring vegetation systems in the Great Plains with ERTS. *Proc. Third ERTS Symp.* 309–317.
- Schuster, C., Förster, M., Kleinschmit, B., 2012. Testing the red edge channel for improving land-use classifications based on high-resolution multi-spectral satellite data. *Int. J. Remote Sens.* 33, 5583–5599. <https://doi.org/10.1080/01431161.2012.666812>.
- Shannon, C.E., 1948. A mathematical theory of communication. *Bell Syst. Tech. J.* 27, 379–423.
- Small, C., 2004. The Landsat ETM+ spectral mixing space. *Remote Sens. Environ.* 93, 1–17. <https://doi.org/10.1016/j.rse.2004.06.007>.
- Vihervaaara, P., Auvinen, A., Pekka, Mononen, Laura, Törmä, Markus, Ahlroth, Petri, Anttila, Saku, Böttcher, Kristin, Forsius, Martin, Heino, Jani, Heliölä, Janne, Koskelainen, Meri, Kuussaari, Mikko, Meissner, Kristian, Ojala, Olli, Tuominen, Seppo, Viitasalo, Markku, Virkkala, R., 2017. How essential biodiversity variables and remote sensing can help national biodiversity monitoring. *Glob. Ecol. Conserv.* 10, 43–59. <https://doi.org/10.1016/j.gecco.2017.01.007>.
- Viña, A., Gitelson, A.A., 2005. New developments in the remote estimation of the fraction of absorbed photosynthetically active radiation in crops. *Geophys. Res. Lett.* 32, 1–4. <https://doi.org/10.1029/2005GL023647>.
- Wang, R., Gamon, J.A., Cavender-Bares, J., Townsend, P.A., Zyguelbaum, A.I., 2018. The spatial sensitivity of the spectral diversity-biodiversity relationship: an experimental test in a prairie grassland. *Ecol. Appl.* 28 (2), 541–556. <https://doi.org/10.1002/eap.1669>.
- Wang, R., Gamon, J.A., Emmerton, C.A., Li, H., Nestola, E., Pastorello, G.Z., Menzer, O., 2016a. Integrated analysis of productivity and biodiversity in a southern Alberta prairie. *Remote Sens.* 8 (3), 214. <https://doi.org/10.3390/rs8030214>.
- Wang, R., Gamon, J.A., Montgomery, R.A., Townsend, P.A., Zyguelbaum, A.I., Bitan, K., Tilman, D., Cavender-Bares, J., 2016b. Seasonal variation in the NDVI-species richness relationship in a prairie grassland experiment (cedar creek). *Remote Sens.* 8 (2), 128. <https://doi.org/10.3390/rs8020128>.
- Whittaker, R.H., 1972. Evolution and measurement of species diversity. *Taxon* 21, 213–251.
- Woodcock, C.E., Strahler, A.H., 1987. The factor of scale in remote sensing. *Remote Sens. Environ.* 21, 311–332. [https://doi.org/10.1016/0034-4257\(87\)90015-0](https://doi.org/10.1016/0034-4257(87)90015-0).